

Urban scale spatial  
patterns of the NO<sub>2</sub>  
Column

L. C. Valin et al.

This discussion paper is/has been under review for the journal Atmospheric Chemistry and Physics (ACP). Please refer to the corresponding final paper in ACP if available.

# Chemical feedback effects on the spatial patterns of the NO<sub>x</sub> weekend effect: a sensitivity analysis

L. C. Valin<sup>1,\*</sup>, A. R. Russell<sup>1,\*\*</sup>, and R. C. Cohen<sup>1,2</sup>

<sup>1</sup>College of Chemistry, University of California Berkeley, Berkeley, CA 94720, USA

<sup>2</sup>Department of Earth and Planetary Sciences, University of California Berkeley, Berkeley, CA 94720, USA

\*now at: Lamont-Doherty Earth Observatory, Columbia University, Palisades, NY 10964, USA

\*\*now at: Sonoma Technology, Inc., Petaluma, CA 94954, USA

Received: 17 April 2013 – Accepted: 20 June 2013 – Published: 19 July 2013

Correspondence to: R. C. Cohen (rccohen@berkeley.edu)

Published by Copernicus Publications on behalf of the European Geosciences Union.

Title Page

Abstract

Introduction

Conclusions

References

Tables

Figures

◀

▶

◀

▶

Back

Close

Full Screen / Esc

Printer-friendly Version

Interactive Discussion



## Abstract

We examine spatial variations in the day-of-week pattern of  $\text{NO}_2$  over the Los Angeles metropolitan area using the Ozone Monitoring Instrument (OMI) and then compare the observations to calculations using the WRF-Chem model. We find that the spatial pattern of the day-of-week variations of the  $\text{NO}_2$  column in the model is significantly different than observed. A sensitivity study shows that the contrasting spatial pattern of  $\text{NO}_2$  on weekdays and weekends is a useful diagnostic of emissions and chemistry and suggest that constraints from space-based observations on the processes affecting urban photochemistry (e.g. spatial patterns of emissions, ratios of VOC to  $\text{NO}_x$  emissions, rate constants) are possible at a level of detail not previously described.

## 1 Introduction

In the troposphere,  $\text{NO}_x$  ( $\text{NO} + \text{NO}_2$ ) affects ozone production rates, aerosol formation and the oxidative capacity of the atmosphere.  $\text{NO}_x$  is emitted to the troposphere by fossil-fuel combustion, biomass burning, soil microbial processes, and lightning. During the daytime  $\text{NO}_x$  is removed from the atmosphere by reactions of  $\text{HO}_x$  ( $\text{OH} + \text{HO}_2 + \text{RO}_2$ ) with  $\text{NO}_x$ , primarily by reaction of OH with  $\text{NO}_2$  to form nitric acid,  $\text{RC}(\text{O})\text{O}_2$  with  $\text{NO}_2$  to form acylperoxy nitrates, and  $\text{RO}_2$  with NO to form alkyl nitrates. As a result, the chemical removal of  $\text{NO}_x$  depends on the concentration of OH and the local mix of volatile organic compound (VOC) precursors to  $\text{RC}(\text{O})\text{O}_2$  and  $\text{RO}_2$  (e.g., Browne and Cohen, 2012). Both OH and  $\text{RO}_2$  depend non-linearly on  $\text{NO}_x$  introducing a powerful nonlinear feedback of  $\text{NO}_x$  on its own lifetime (Fig. 1).

Satellite-based observation of the  $\text{NO}_2$  column has provided a wealth of information on  $\text{NO}_x$  at local (e.g., Bertram et al., 2005; Boersma et al., 2009; Russell et al., 2012), regional (e.g., Richter et al., 2005; Kim et al., 2009; Hudman et al., 2010), and global scales (e.g., Stavrou et al., 2008; Lamsal et al., 2011) proving particularly useful for study of seasonal (Jaeglé et al., 2005; van der A et al., 2006), interannual (e.g., Richter

ACPD

13, 19173–19192, 2013

## Urban scale spatial patterns of the $\text{NO}_2$ Column

L. C. Valin et al.

Title Page

Abstract

Introduction

Conclusions

References

Tables

Figures

◀

▶

◀

▶

Back

Close

Full Screen / Esc

Printer-friendly Version

Interactive Discussion



**Urban scale spatial patterns of the NO<sub>2</sub> Column**

L. C. Valin et al.

Title Page

Abstract

Introduction

Conclusions

References

Tables

Figures

◀

▶

◀

▶

Back

Close

Full Screen / Esc

Printer-friendly Version

Interactive Discussion



et al., 2005; van der A et al., 2008; Russell et al., 2012), and day-of-week (e.g., Beirle et al., 2003; Kaynak et al., 2009; Russell et al., 2010) trends in NO<sub>2</sub> column. Typically, the observed columns and their trends are used to assess differences in NO<sub>x</sub> emissions (e.g., Beirle et al., 2003; Kim et al., 2006). In situ observations (e.g., Thornton et al., 2002; Murhpy et al., 2007) have provided extensive information on the mechanistic details affecting the NO<sub>x</sub> lifetime on weekdays and weekends, but lack the coverage in space and time of space-based measurements. With a nadir footprint of 13 km × 24 km and daily, global coverage, the Ozone Monitoring Instrument (OMI – Levelt et al., 2006) provides coverage and spatial detail at a scale relevant to boundary layer NO<sub>x</sub> removal (~ 10–50 km; e.g., Ryerson et al., 2001; Dillon et al., 2002; Beirle et al., 2011; Valin et al., 2011a,b). Recently OMI observations have been shown to be sensitive not only to NO<sub>x</sub> emissions but also to provide constraints on the NO<sub>x</sub> lifetime and its variation with wind speed (e.g., Valin et al., 2013).

Here, we use OMI observations to describe the spatial variation of the NO<sub>2</sub> column over Los Angeles on weekends and weekdays. We then use a series of WRF-Chem model simulations in a sensitivity study to characterize the information contained in the day-of-week patterns. From the range of simulations computed, we identify modifications to the base model that produce improved matches to the spatial pattern OMI observations and use this to guide our understanding of the chemical processes that control the NO<sub>2</sub> column.

## 2 Observations

The Ozone Monitoring Instrument (OMI), a UV/VIS spectrometer developed at KNMI in the Netherlands (Levelt et al., 2006), is mounted on the polar-orbiting, sun-synchronous NASA Aura satellite (Schoerbl et al., 2006). OMI has a 114° field-of-view, with 480 detector elements devoted to spatial coverage that are averaged onboard to provide 60 pixels across a 2600 km swath of the earth, and a 2 s integration period that results in a 13 km pixel dimension in the direction of the spacecraft motion. The resulting spatial

footprint is as small as 13 km × 24 km. Aura/OMI orbits the earth over 14 times a day providing near global coverage at approximately 1.15 p.m. local solar time.

Several different analyses of the spectrum measured by OMI are publically available (Bucsela et al., 2006; Boersma et al., 2007; Russell et al., 2011). Here, we use the BErkeley High Resolution (BEHR) retrieval of OMI NO<sub>2</sub> vertical tropospheric columns (available at <http://behr.cchem.berkeley.edu> – Russell et al., 2011, 2012). Briefly, BEHR derives tropospheric vertical NO<sub>2</sub> column from the NASA standard tropospheric slant column (Bucsela et al., 2006) using high spatial resolution inputs to the Standard Product AMF lookup table, specifically 12 km × 12 km monthly-averaged vertical NO<sub>2</sub> profiles, 0 : 05° × 0 : 05° 16 day average MODIS albedo product (MCD43C3), and the Global Land One-kilometer Base Elevation (GLOBE) Digital Elevation Model. Here, we use BEHR version 1.0B. The version number corresponds to the version of the Standard Product used to derive BEHR, and the version letter corresponds to the version of BEHR for a given Standard Product version

Figure 2 shows the average May–July 2005–2007 weekday NO<sub>2</sub> column (Monday–Friday), the weekend column (Saturday–Sunday), and the pattern of weekend NO<sub>2</sub> column decreases observed by OMI over Southern California. We include a true-color Aqua-MODIS image of the region observed on a cloud-free day (29 May 2005). The Greater Los Angeles metropolitan area consists of three distinct basins: the Los Angeles Basin at the coast (33.8°–34.1° N, 117.8°–118.4° W), the San Fernando Valley to the northwest (34.1°–34.3° N, 118.2°–118.8° W), and the San Bernardino Valley to the East (33.8°–34.2° N, 117.0°–117.8° W). During the summer, the typical daytime meteorology consists of onshore flow entering the Los Angeles basin at the coast flowing out through the San Bernardino Valley to the east and the San Fernando Valley to the northwest.

Due to the onshore flow and large coastal emission sources, the weekday NO<sub>2</sub> column increases sharply at the coastline to a maximum of  $3.9 \times 10^{16}$  molecules cm<sup>-2</sup> directly over downtown Los Angeles (Fig. 1b). In the San Bernardino Valley, NO<sub>2</sub> columns decrease gradually. Decreases in the San Fernando Valley are sharper than in San

## Urban scale spatial patterns of the NO<sub>2</sub> Column

L. C. Valin et al.

Title Page

Abstract

Introduction

Conclusions

References

Tables

Figures

◀

▶

◀

▶

Back

Close

Full Screen / Esc

Printer-friendly Version

Interactive Discussion



Bernardino. Over a long-term average the airflow on weekends is identical to that on weekdays. The weekend  $\text{NO}_2$  column is markedly lower than the weekday column and the gradients downwind of central Los Angeles are much steeper. Weekend decreases of the  $\text{NO}_2$  column are only 25–40 % over coastal and downtown Los Angeles but are 45–55 % over the San Fernando Valley and an even larger 55–65 % over the San Bernardino Valley.

Large decreases of the  $\text{NO}_2$  column and surface concentration on weekends have been reported previously using satellite and in situ observations (e.g., Beirle et al., 2003; Murphy et al., 2007; Russell et al., 2010). The changes have been attributed primarily to a day-of-week pattern of emissions, with decreases in the US associated with a reduction in freight transport by heavy-duty diesel powered vehicles (Harley et al., 2005). However, these decreases in emissions result in decreases in  $\text{NO}_x$  concentrations that affect the  $\text{NO}_x$  lifetime through the chemical feedbacks on OH and  $\text{O}_3$  (e.g., Valin et al., 2011b; Stephens et al., 2008; Pollack et al., 2012; Pusede and Cohen, 2012 and references therein). Previously, analyses have largely assumed changes associated with emissions and the feedbacks are uniform across an urban center (Beirle et al., 2003; Brioude et al., 2013). The observation that the  $\text{NO}_2$  decreases are not spatially uniform has not, to our knowledge, been previously reported or evaluated in a model. In the following, we simulate the day-of-week pattern of  $\text{NO}_2$  column using WRF-Chem and compare the results to the observations in an effort to understand which model parameters are important for describing the day-of-week patterns in Los Angeles, and by analogy, for describing day-of-week patterns of  $\text{NO}_2$  in other locations. Our goal is not to produce exact agreement but rather to illustrate that the spatial pattern of observations contains information that can provide new constraints on our understanding of urban photochemistry and emissions.

## Urban scale spatial patterns of the $\text{NO}_2$ Column

L. C. Valin et al.

[Title Page](#)[Abstract](#)[Introduction](#)[Conclusions](#)[References](#)[Tables](#)[Figures](#)[Back](#)[Close](#)[Full Screen / Esc](#)[Printer-friendly Version](#)[Interactive Discussion](#)

### 3 WRF-Chem calculations

We simulate the  $\text{NO}_2$  column at the OMI overpass time (1 p.m.) using WRF-Chem (Grell et al., 2005) at 4 km horizontal resolution over a 288 km (N–S) by 480 km (E–W) domain, centered at  $34^\circ\text{N}$ ,  $118^\circ\text{W}$ . We use 36 vertical layers, 14 of which are in the first 1.5 km. As our base case, we use the Regional Acid Deposition Model 2 (RADM2) chemical mechanism, the 2005 National Emissions Inventory (NEI2005) for anthropogenic emissions and the default online module for biogenic emissions as in Grell et al. (2005). Initial and boundary conditions for meteorology are taken from the North American Regional Reanalysis (NARR) and for chemistry are taken from an idealized profile standard to WRF-Chem.

We simulate the average 1 p.m.  $\text{NO}_2$  column for 1–14 June 2008 with NEI2005 anthropogenic emissions (weekday) and the same model with an emission rate of  $0.625 \cdot E_{\text{NO}_x\text{-NEI2005}}$  (weekend). The first two days are used as spin-up. For the base case, we run WRF-Chem with standard RADM2 chemistry and spatially and temporally uniform weekend emission reductions. We compare results from this base case calculation to weekday/weekend simulations in which we adjust  $\text{HO}_x$  production from ozone photolysis ( $0.5\times$ ,  $1.25\times$ ,  $1.5\times$ ,  $2\times$ ), VOC emissions ( $0.5\times$ ,  $2\times$ ), VOC–OH rate constants ( $0.5\times$ ,  $2\times$ ), the  $\text{NO}_2$ –OH rate constant ( $0.5\times$ ,  $2\times$ ), the timing of weekend emissions (1 h delay, 2 h delay), and the spatial distribution of weekend emissions (Weekend  $E_{\text{NO}_x\text{-San Bernardino}} 0.575\times$ ,  $0.525 \times E_{\text{NO}_x\text{-NEI2005}}$ , and  $E_{\text{NO}_x\text{-Los Angeles}} 0.640\times$ ,  $0.654 \times E_{\text{NO}_x\text{-NEI2005}}$ , for domain-average weekend emission of  $0.625 \times E_{\text{NO}_x\text{-NEI2005}}$ ). The results from these simulations and the OMI observations are summarized in Table 1. Table 1 reports the total reduction of  $\text{NO}_2$  column over the entire Los Angeles plume (defined as the area over which the OMI-observed weekday  $\text{NO}_2$  columns exceed  $2.5 \times 10^{15}$  molecules  $\text{cm}^{-2}$ ) and the fraction of the Los Angeles plume with weekend decreases of  $\text{NO}_2$  column that exceed 35 %, 45 %, and 55 %.

We find that the simulated  $\text{NO}_2$  columns, regardless of model scenario, are biased low where  $\text{NO}_2$  is low. To correct this bias we add a regionally uniform background

## Urban scale spatial patterns of the $\text{NO}_2$ Column

L. C. Valin et al.

Title Page

Abstract

Introduction

Conclusions

References

Tables

Figures

◀

▶

◀

▶

Back

Close

Full Screen / Esc

Printer-friendly Version

Interactive Discussion



column of  $5 \times 10^{14}$  molecules  $\text{cm}^{-2}$  to both the weekday and weekend simulations for all model scenarios. This correction does not significantly impact model results where the  $\text{NO}_2$  columns are high, but does alter the simulated spatial patterns at the edges of the plume where  $\text{NO}_2$  is low ( $\sim 20\%$  effect where  $\text{NO}_2$  columns are  $2.5 \times 10^{15}$  molecules  $\text{cm}^{-2}$ ). We test whether a two week period of simulation is representative of longer time periods by simulating the base case scenario for three months and find that the magnitude and pattern of decreases simulated in the two-week scenario is comparable to that of the 3 month scenario indicating its fidelity in representing the meteorological variability of a longer-term simulation. We also test for memory effects by simulating weekday  $\text{NO}_2$  column in two-day periods (3–4 June, 4–5 June, . . . , 13–14 June) initialized with the model  $\text{NO}_2$  column from 4 p.m. LST on the previous weekday to test whether simulation of 14 consecutive weekend days is biased relative to simulation of two-day weekends within a weekly cycle. We find that the memory effect of weekday emissions on weekend column is small compared to the effects of the other parameters tested.

#### 4 Model results and analysis

In Fig. 3, we compare the observed day-of-week pattern of  $\text{NO}_2$  column (top row) to that simulated with the base model (second row). Integrated over the entire basin, there is only a 2% difference between observation and simulation and both exhibit similar spatial patterns. Locally, however, there are large differences between the simulated and observed  $\text{NO}_2$  columns (up to a factor of two). OMI observes much higher  $\text{NO}_2$  values on the south and west edges of the plume, and the model predicts much higher values in the outflow regions, namely the southeast and northwest edges of the plume. This discrepancy indicates several possible model or observational uncertainties. For instance,  $\text{NO}_2$  may be transported downwind too quickly in the model, the observations may be biased over the coastline (e.g., solar glint reflectance impacts on the  $\text{NO}_2$  retrieval), or OMI with its pixels of  $13\text{ km} \times 24\text{ km}$  may be smearing the spatial pattern

### Urban scale spatial patterns of the $\text{NO}_2$ Column

L. C. Valin et al.

Title Page

Abstract

Introduction

Conclusions

References

Tables

Figures

◀

▶

◀

▶

Back

Close

Full Screen / Esc

Printer-friendly Version

Interactive Discussion



that is simulated at a model horizontal resolution of 4 km × 4 km even though our average of the OMI data takes advantage of oversampling to increase the resolution to approximately 10 km × 10 km (e.g., Russell et al., 2010).

The large, localized differences between the observed and simulated NO<sub>2</sub> columns highlight the difficulty of accurately computing the interplay of emissions, chemistry and transport or of accounting for the possibility of locally-specific observational biases. However, when investigating the patterns of NO<sub>2</sub> column (e.g., day-of-week effect) within self-consistent model simulations or observational datasets, many of these biases are eliminated. In our WRF-Chem model setup, for instance, the weekday and weekend meteorology is identical, and over a long time period, OMI observes weekday and weekend NO<sub>2</sub> columns that are subject to the same average meteorological patterns and the same average observational biases. As a result, the agreement of simulated and observed NO<sub>2</sub> trends (e.g, day-of-week effect; Fig. 3 – right column) is more meaningful than the agreement between observations and simulations for a single time period (e.g., weekday NO<sub>2</sub> column; Fig. 3 – left column). In the base model, simulated NO<sub>2</sub> decreases are too large over the coast (40 % vs. 30 %), are too small over San Bernardino (50 % vs. 60 %), and extend too far inland (150 km vs. 100 km).

The day-of-week pattern of the NO<sub>2</sub> column depends both on patterns of NO<sub>x</sub> removal and patterns of NO<sub>x</sub> emissions. The pattern of removal depends on the relationship of OH and RO<sub>2</sub> concentrations to NO<sub>x</sub> (Fig. 1). In Los Angeles, where NO<sub>x</sub> concentrations are high (i.e., to the right side of the NO<sub>x</sub>-OH curve), a decrease of NO<sub>x</sub> emissions on the weekends results in higher concentrations of OH and RO<sub>2</sub>. As a result, NO<sub>x</sub> is removed faster, and the reduction of NO<sub>2</sub> columns on the weekend is larger than the reduction of NO<sub>x</sub> emissions alone. The spatial map of these nonlinear effects reflects the timescale for NO<sub>x</sub> removal (Fig. 3 – right column). If the chemical removal of NO<sub>x</sub> is slow, the nonlinear decreases will be small over the source where NO<sub>x</sub> concentrations are high, but will persist and accumulate far downwind where the concentrations eventually decrease to a value that corresponds to a maximum OH concentration and a minimum in the NO<sub>x</sub> chemical lifetime (Fig. 1). If the chemical removal

## Urban scale spatial patterns of the NO<sub>2</sub> Column

L. C. Valin et al.

Title Page

Abstract

Introduction

Conclusions

References

Tables

Figures

⏪

⏩

◀

▶

Back

Close

Full Screen / Esc

Printer-friendly Version

Interactive Discussion



of  $\text{NO}_x$  is rapid near the source, the nonlinear feedbacks will be large in that location. The discrepancy between the observations and the base simulation (Fig. 3 – first row vs. second row) suggests that the model falls into the first category while the observations fall into the second category, an indication that the simulated OH and  $\text{RO}_2$  concentrations are too low (i.e., the model is too far to the right of the  $\text{NO}_2$ -OH curve presented in Fig. 1).

To test this hypothesis, we evaluate the effects of parameters that influence the concentration of OH and  $\text{RO}_2$ , and thus affect the timescale of  $\text{NO}_x$  removal. We double the rate of ozone photolysis to increase the concentration of OH and  $\text{RO}_2$  (i.e. shift the entire  $\text{NO}_2$ -OH curve in Fig. 1 upward). Separately, we double the anthropogenic emissions of VOC to increase the concentration of  $\text{RO}_2$  throughout the model domain.

Figure 3 (third row) shows the simulated day-of-week pattern of the  $\text{NO}_2$  column when  $\text{HO}_x$  production is increased. Due to the increase of  $\text{HO}_x$ , the rate of  $\text{NO}_x$  removal increases, and both weekday and weekend  $\text{NO}_2$  columns are smaller than those simulated in the base model. As a result of higher OH and  $\text{RO}_2$ , the timescale of  $\text{NO}_x$  losses is shortened compared to the timescale of transport, and, as hypothesized, the weekend decrease is larger near the source and does not extend as far downwind relative to the base case. Here, we adjust  $\text{HO}_x$  production using ozone photolysis, but other sources of  $\text{HO}_x$  (or Cl), such as HONO,  $\text{ClNO}_2$ , or HCHO photolysis may play a role.

Figure 3 (fourth row) shows the simulated day-of-week pattern of the  $\text{NO}_2$  column when VOC emissions are doubled. VOC both removes OH and leads to OH formation through its feedback on  $\text{HO}_x$  sources (e.g.,  $\text{O}_3$ , formaldehyde). At low  $\text{NO}_x$  concentrations, the role of VOC as a sink of OH dominates, and OH decreases for any increase of VOC. At high  $\text{NO}_x$ , however, the role of VOC as a sink of OH is small, and the concentration of OH increases with increases of VOC. As a result,  $\text{RO}_2$  increases everywhere for an increase of VOC emissions, and OH increases where  $\text{NO}_x$  is high ( $\text{NO}_2$  column  $> 7.5 \times 10^{15}$  molecule  $\text{cm}^{-2}$ ) but decreases where  $\text{NO}_x$  is low ( $\text{NO}_2$  column  $< 5 \times 10^{15}$  molecule  $\text{cm}^{-2}$ ). Due to higher OH and  $\text{RO}_2$  concentrations over Los

**Urban scale spatial patterns of the  $\text{NO}_2$  Column**

L. C. Valin et al.

Title Page

Abstract

Introduction

Conclusions

References

Tables

Figures

◀

▶

◀

▶

Back

Close

Full Screen / Esc

Printer-friendly Version

Interactive Discussion



Angeles, the timescale of  $\text{NO}_2$  removal is shortened when VOC emissions are increased relative to the base model, and the agreement of the simulated day-of-week pattern with observations improves. Here, we alter VOC concentrations by altering anthropogenic VOC emissions, but biogenic emissions may also be a significant source of VOC in Los Angeles.

The comparison of modeled and observed day-of-week patterns of the  $\text{NO}_2$  column suggest that  $\text{HO}_x$  chemistry in Los Angeles is  $\text{NO}_x$ -saturated (Fig. 1), but also indicate that the Los Angeles atmosphere is not as far to the right of the  $\text{NO}_x$ -OH- $\text{RO}_2$  relationship as the model simulation. We find that agreement between model and observation is improved when we increase  $\text{HO}_x$  production or VOC emissions in the model, but the improvement is similar for both changes (Fig. 3 – third row vs. fourth row). Despite their similarities, there are significant differences between these two adjustments, particularly differences in the relative roles of  $\text{RO}_2$  and OH as  $\text{NO}_x$  sinks (i.e., PAN and  $\text{RONO}_2$  vs.  $\text{HNO}_3$ ). PAN, for example, is thermally unstable and is much more likely to re-release  $\text{NO}_x$  downwind than is  $\text{HNO}_3$ , which is more likely to deposit before undergoing photolysis or reaction with OH. Distinguishing the roles of  $\text{HNO}_3$  and PAN chemistry may require more information, such as higher spatial resolution satellite-based measurements at the plume edges where the differences between the two simulations seem the largest or time resolved measurements as will become available from geostationary orbit (e.g., GEO-CAPE – Fishman et al., 2008).

The day-of-week pattern of  $\text{NO}_2$  columns also depends on day-of-week patterns of emissions. The timing of emissions shifts later in the day on weekends (Harley et al., 2005). The delay of emissions on weekends relative to weekdays is expected from a shift of light-duty gasoline vehicle activity later in the day. Weekend emission reductions also vary regionally, and likely locally, due to differing day-of-week trends in industry and heavy-duty diesel truck activity relative to passenger vehicle activity (McDonald et al., 2012).

Figure 3 (fifth row) shows the day-of-week pattern of  $\text{NO}_2$  simulated when we delay the timing of all weekend emissions, both VOC and  $\text{NO}_x$ , by two hours. When weekend

## Urban scale spatial patterns of the $\text{NO}_2$ Column

L. C. Valin et al.

Title Page

Abstract

Introduction

Conclusions

References

Tables

Figures

◀

▶

◀

▶

Back

Close

Full Screen / Esc

Printer-friendly Version

Interactive Discussion



emissions are delayed, the 1 p.m.  $\text{NO}_2$  column decreases because the total emissions in the hours prior to the satellite overpass decrease. The timing of emissions affects the magnitude of the observed decreases but does not significantly affect the spatial pattern.

Figure 3 (sixth row) shows the day-of-week pattern of  $\text{NO}_2$  calculated with a different weekend emission reduction over San Bernardino ( $0.525 \times E_{\text{NO}_x\text{-NEI2005}}$ ) than over Los Angeles ( $0.654 \times E_{\text{NO}_x\text{-NEI2005}}$ ) where the total weekend emission reduction is no different than the base case ( $0.625 \times E_{\text{NO}_x\text{-NEI2005}}$ ). Not surprisingly, the contrast between the East basin (San Bernardino) and the West basin (Los Angeles) is larger when the regional day-of-week emission pattern is altered, a modest effect, but one that is consistent with observations that show larger decreases over San Bernardino and smaller decreases over the Los Angeles basin. This pattern might be used in conjunction with detailed vehicle activity assessments to understand whether the changes are consistent with a differential weekend decrease of heavy-duty diesel truck traffic in the two regions.

In the set of simulations discussed above, we show that the  $\text{NO}_2$  column and more specifically day-of-week patterns of  $\text{NO}_2$  column depend strongly on  $\text{HO}_x$  production, VOC, and the timing and spatial distribution of weekend emissions. While no single modification provides an unbiased representation of the observed day-of-week pattern over Los Angeles, our comparison of the simulated and observed patterns provides a framework for future work aimed at optimally reproducing the day-of-week pattern of  $\text{NO}_2$  column over Los Angeles or any location.

## 5 Conclusions

The high spatial resolution of OMI ( $13 \text{ km} \times 24 \text{ km}$ ) captures a phenomenal level of detail over the Los Angeles metropolitan area ( $200 \text{ km} \times 150 \text{ km}$ ). Comparisons of these observations to a high resolution model demonstrate that this spatial detail provides information on local patterns of  $\text{NO}_x$  transport, emissions and chemistry. The obser-

### Urban scale spatial patterns of the $\text{NO}_2$ Column

L. C. Valin et al.

Title Page

Abstract

Introduction

Conclusions

References

Tables

Figures

⏪

⏩

◀

▶

Back

Close

Full Screen / Esc

Printer-friendly Version

Interactive Discussion





**Urban scale spatial patterns of the NO<sub>2</sub> Column**

L. C. Valin et al.

Title Page

Abstract

Introduction

Conclusions

References

Tables

Figures

◀

▶

◀

▶

Back

Close

Full Screen / Esc

Printer-friendly Version

Interactive Discussion

- Beirle, S., Boersma, K. F., Platt, U., Lawrence, M. G., and Wagner, T.: Megacity emissions and lifetimes of nitrogen oxides probed from space, *Science*, 333, 1737–1739, doi:10.1126/science.1207824, 2011.
- Bertram, T. H., Heckel, A., Richter, A., Burrows, J. P., and Cohen, R. C.: Satellite measurements of daily variations in soil NO<sub>x</sub> emissions, *Geophys. Res. Lett.*, 32, L24812, doi:10.1029/2005GL024640, 2005.
- Boersma, K. F., Eskes, H. J., Veefkind, J. P., Brinksma, E. J., van der A, R. J., Sneep, M., van den Oord, G. H. J., Levelt, P. F., Stammes, P., Gleason, J. F., and Bucsela, E. J.: Near-real time retrieval of tropospheric NO<sub>2</sub> from OMI, *Atmos. Chem. Phys.*, 7, 2103–2118, doi:10.5194/acp-7-2103-2007, 2007.
- Boersma, K. F., Jacob, D. J., Trainic, M., Rudich, Y., DeSmedt, I., Dirksen, R., and Eskes, H. J.: Validation of urban NO<sub>2</sub> concentrations and their diurnal and seasonal variations observed from the SCIAMACHY and OMI sensors using in situ surface measurements in Israeli cities, *Atmos. Chem. Phys.*, 9, 3867–3879, doi:10.5194/acp-9-3867-2009, 2009.
- Brioude, J., Angevine, W. M., Ahmadov, R., Kim, S.-W., Evan, S., McKeen, S. A., Hsie, E.-Y., Frost, G. J., Neuman, J. A., Pollack, I. B., Peischl, J., Ryerson, T. B., Holloway, J., Brown, S. S., Nowak, J. B., Roberts, J. M., Wofsy, S. C., Santoni, G. W., Oda, T., and Trainer, M.: Top-down estimate of surface flux in the Los Angeles Basin using a mesoscale inverse modeling technique: assessing anthropogenic emissions of CO, NO<sub>x</sub> and CO<sub>2</sub> and their impacts, *Atmos. Chem. Phys.*, 13, 3661–3677, doi:10.5194/acp-13-3661-2013, 2013.
- Browne, E. C. and Cohen, R. C.: Effects of biogenic nitrate chemistry on the NO<sub>x</sub> lifetime in remote continental regions, *Atmos. Chem. Phys.*, 12, 11917–11932, doi:10.5194/acp-12-11917-2012, 2012.
- Bucsela, E. J., Celarier, E. A., Wenig, M. O., Gleason, J. F., Veefkind, J. P., Boersma, K. F., and Brinksma, E. J.: Algorithm for NO<sub>2</sub> vertical column retrieval from the ozone monitoring instrument, *IEEE Trans. Geosci. Remote Sens.*, 44, 1245–1258, doi:10.1109/tgrs.2005.863715, 2006.
- Dillon, M. B., Lamanna, M. S., Schade, G. W., Goldstein, A. H., and Cohen, R. C.: Chemical evolution of the Sacramento urban plume: transport and oxidation, *J. Geophys. Res.-Atmos.*, 107, ACH 3-1-ACH 3-15, doi:10.1029/2001jd000969, 2002.
- Fishman, J., Bowman, K. W., Burrows, J. P., Richter, A., Chance, K. V., Edwards, D. P., Martin, R. V., Morris, G. A., Pierce, R. B., Ziemke, J. R., Al-Saadi, J. A., Creilson, J. K.,

**Urban scale spatial  
patterns of the NO<sub>2</sub>  
Column**

L. C. Valin et al.

Title Page

Abstract

Introduction

Conclusions

References

Tables

Figures

◀

▶

◀

▶

Back

Close

Full Screen / Esc

Printer-friendly Version

Interactive Discussion



Schaack, T. K., and Thompson, A. M.: Remote sensing of tropospheric pollution from space, *B. Am. Meteorol. Soc.*, 89, 805–821, doi:10.1175/2008bams2526.1, 2008.

Grell, G. A., Peckham, S. E., Schmitz, R., McKeen, S. A., Frost, G., Skamarock, W. C., and Eder, B.: Fully coupled “online” chemistry within the WRF model, *Atmos. Environ.*, 39, 6957–6975, doi:10.1016/j.atmosenv.2005.04.027, 2005.

Harley, R. A., Marr, L. C., Lehner, J. K., and Giddings, S. N.: Changes in motor vehicle emissions on diurnal to decadal time scales and effects on atmospheric composition, *Environ. Sci. Tech.*, 39, 5356–5362, doi:10.1021/es048172+, 2005.

Hudman, R. C., Russell, A. R., Valin, L. C., and Cohen, R. C.: Interannual variability in soil nitric oxide emissions over the United States as viewed from space, *Atmos. Chem. Phys.*, 10, 9943–9952, doi:10.5194/acp-10-9943-2010, 2010.

Jaeglé, L., Steinberger, L., Martin, R. V., and Chance, K.: Global partitioning of NO<sub>x</sub> sources using satellite observations: relative roles of fossil fuel combustion, biomass burning and soil emissions, *Faraday Disc.*, 130, 407–423, doi:10.1039/B502128F, 2005.

Kaynak, B., Hu, Y., Martin, R. V., Sioris, C. E., and Russell, A. G.: Comparison of weekly cycle of NO<sub>2</sub> satellite retrievals and NO<sub>x</sub> emission inventories for the continental United States, *J. Geophys. Res.-Atmos.*, 114, D05302, doi:10.1029/2008JD010714, 2009.

Kim, S. W., Heckel, A., McKeen, S. A., Frost, G. J., Hsie, E. Y., Trainer, M. K., Richter, A., Burrows, J. P., Peckham, S. E., and Grell, G. A.: Satellite-observed US power plant NO<sub>x</sub> emission reductions and their impact on air quality, *Geophys. Res. Lett.*, 33, 5, L22812, doi:10.1029/2006GL027749, 2006.

Kim, S. W., Heckel, A., Frost, G. J., Richter, A., Gleason, J., Burrows, J. P., McKeen, S., Hsie, E. Y., Granier, C., and Trainer, M.: NO<sub>2</sub> columns in the western United States observed from space and simulated by a regional chemistry model and their implications for NO<sub>x</sub> emissions, *J. Geophys. Res.-Atmos.*, 114, 29, D11301, doi:10.1029/2008JD011343, 2009.

Lamsal, L. N., Martin, R. V., Padmanabhan, A., van Donkelaar, A., Zhang, Q., Sioris, C. E., Chance, K., Kurosu, T. P., and Newchurch, M. J.: Application of satellite observations for timely updates to global anthropogenic NO<sub>x</sub> emission inventories, *Geophys. Res. Lett.*, 38, L05810, doi:10.1029/2010gl046476, 2011.

Levelt, P. F., Van den Oord, G. H. J., Dobber, M. R., Malkki, A., Visser, H., de Vries, J., Stammes, P., Lundell, J. O. V., and Saari, H.: The ozone monitoring instrument, *IEEE Trans. Geosci. Remote Sens.*, 44, 1093–1101, doi:10.1109/tgrs.2006.872333, 2006.

**Urban scale spatial  
patterns of the NO<sub>2</sub>  
Column**

L. C. Valin et al.

Title Page

Abstract

Introduction

Conclusions

References

Tables

Figures

◀

▶

◀

▶

Back

Close

Full Screen / Esc

Printer-friendly Version

Interactive Discussion



McDonald, B. C., Dallmann, T. R., Martin, E. W., and Harley, R. A.: Long-term trends in nitrogen oxide emissions from motor vehicles at national, state, and air basin scales, *J. Geophys. Res.*, 117, D00V18, doi:10.1029/2012JD018304, 2012.

Murphy, J. G., Day, D. A., Cleary, P. A., Wooldridge, P. J., Millet, D. B., Goldstein, A. H., and Cohen, R. C.: The weekend effect within and downwind of Sacramento – Part 1: Observations of ozone, nitrogen oxides, and VOC reactivity, *Atmos. Chem. Phys.*, 7, 5327–5339, doi:10.5194/acp-7-5327-2007, 2007.

Pollack, I. B., Ryerson, T. B., Trainer, M., Parrish, D. D., Andrews, A. E., Atlas, E. L., Blake, D. R., Brown, S. S., Commane, R., Daube, B. C., de Gouw, J. A., Dube, W. P., Flynn, J., Frost, G. J., Gilman, J. B., Grossberg, N., Holloway, J. S., Kofler, J., Kort, E. A., Kuster, W. C., Lang, P. M., Lefer, B., Lueb, R. A., Neuman, J. A., Nowak, J. B., Novelli, P. C., Peischl, J., Perring, A. E., Roberts, J. M., Santoni, G., Schwarz, J. P., Spackman, J. R., Wagner, N. L., Warneke, C., Washenfelder, R. A., Wofsy, S. C., and Xiang, B.: Airborne and ground-based observations of a weekend effect in ozone, precursors, and oxidation products in the California South Coast Air Basin, *J. Geophys. Res.-Atmos.*, 117, D00V05, doi:10.1029/2011jd016772, 2012.

Pusede, S. E. and Cohen, R. C.: On the observed response of ozone to NO<sub>x</sub> and VOC reactivity reductions in San Joaquin Valley California 1995–present, *Atmos. Chem. Phys.*, 12, 8323–8339, doi:10.5194/acp-12-8323-2012, 2012.

Richter, A., Burrows, J. P., Nuss, H., Granier, C., and Niemeier, U.: Increase in tropospheric nitrogen dioxide over China observed from space, *Nature*, 437, 129–132, doi:10.1038/nature04092, 2005.

Russell, A. R., Valin, L. C., Bucsela, E. J., Wenig, M. O., and Cohen, R. C.: Space-based constraints on spatial and temporal patterns of NO<sub>x</sub> emissions in California, 2005–2008, *Environ. Sci. Tech.*, 44, 3608–3615, doi:10.1021/es903451j, 2010.

Russell, A. R., Perring, A. E., Valin, L. C., Bucsela, E. J., Browne, E. C., Wooldridge, P. J., and Cohen, R. C.: A high spatial resolution retrieval of NO<sub>2</sub> column densities from OMI: method and evaluation, *Atmos. Chem. Phys.*, 11, 8543–8554, doi:10.5194/acp-11-8543-2011, 2011.

Russell, A. R., Valin, L. C., and Cohen, R. C.: Trends in OMI NO<sub>2</sub> observations over the United States: effects of emission control technology and the economic recession, *Atmos. Chem. Phys.*, 12, 12197–12209, doi:10.5194/acp-12-12197-2012, 2012.

Ryerson, T. B., Trainer, M., Holloway, J. S., Parrish, D. D., Huey, L. G., Sueper, D. T., Frost, G. J., Donnelly, S. G., Schauffler, S., Atlas, E. L., Kuster, W. C., Goldan, P. D., Hubler, G., Meagher, J. F., and Fehsenfeld, F. C.: Observations of ozone formation in

## Urban scale spatial patterns of the NO<sub>2</sub> Column

L. C. Valin et al.

Title Page

Abstract

Introduction

Conclusions

References

Tables

Figures

◀

▶

◀

▶

Back

Close

Full Screen / Esc

Printer-friendly Version

Interactive Discussion



power plant plumes and implications for ozone control strategies, *Science*, 292, 719–723, doi:10.1126/science.1058113, 2001.

Schoeberl, M., Douglass, A., Hilsenrath, E., Bhartia, P., Beer, R., Waters, J., Gunson, M., Froidevaux, L., Gille, J., Barnett, J., Levelt, P., and DeCola, P.: Overview of the EOS aura mission, *IEEE Trans. Geosci. Remote Sens.*, 44, 1066–1074, doi:10.1109/tgrs.2005.861950, 2006.

Stavrakou, T., Muller, J. F., Boersma, K. F., De Smedt, I., and van der A, R. J.: Assessing the distribution and growth rates of NO<sub>x</sub> emission sources by inverting a 10-year record of NO<sub>2</sub> satellite columns, *Geophys. Res. Lett.*, 35, L10801, doi:10.1029/2008gl033521, 2008.

Stephens, S., Madronich, S., Wu, F., Olson, J. B., Ramos, R., Retama, A., and Muñoz, R.: Weekly patterns of México City's surface concentrations of CO, NO<sub>x</sub>, PM<sub>10</sub> and O<sub>3</sub> during 1986–2007, *Atmos. Chem. Phys.*, 8, 5313–5325, doi:10.5194/acp-8-5313-2008, 2008.

Thornton, J. A., Wooldridge, P. J., Cohen, R. C., Martinez, M., Harder, H., Brune, W. H., Williams, E. J., Roberts, J. M., Fehsenfeld, F. C., Hall, S. R., Shetter, R. E., Wert, B. P., and Fried, A.: Ozone production rates as a function of NO<sub>x</sub> abundances and HO<sub>x</sub> production rates in the Nashville urban plume, *J. Geophys. Res.-Atmos.*, 107, 4146, doi:10.1029/2001JD000932, 2002.

Valin, L. C., Russell, A. R., Bucsela, E. J., Veefkind, J. P., and Cohen, R. C.: Observation of slant column NO<sub>2</sub> using the super-zoom mode of AURA-OMI, *Atmos. Meas. Tech.*, 4, 1929–1935, doi:10.5194/amt-4-1929-2011, 2011a.

Valin, L. C., Russell, A. R., Hudman, R. C., and Cohen, R. C.: Effects of model resolution on the interpretation of satellite NO<sub>2</sub> observations, *Atmos. Chem. Phys.*, 11, 11647–11655, doi:10.5194/acp-11-11647-2011, 2011b.

Valin, L. C., Russell, A. R., and Cohen, R. C.: Variations of OH radical in an urban plume inferred from NO<sub>2</sub> column measurements, *Geophys. Res. Lett.*, 40, 1856–1860, doi:10.1002/grl.50267, 2013.

van der A, R. J., Peters, D., Eskes, H., Boersma, K. F., Van Roozendael, M., De Smedt, I., and Kelder, H. M.: Detection of the trend and seasonal variation in tropospheric NO<sub>2</sub> over China, *J. Geophys. Res.-Atmos.*, 111, D12317, doi:10.1029/2005JD006594, 2006.

van der A, R. J., Eskes, H. J., Boersma, K. F., van Noije, T. P. C., Van Roozendael, M., De Smedt, I., Peters, D., and Meijer, E. W.: Trends, seasonal variability and dominant NO<sub>x</sub> source derived from a ten year record of NO<sub>2</sub> measured from space, *J. Geophys. Res.-Atmos.*, 113, D04302, doi:10.1029/2007JD009021, 2008.



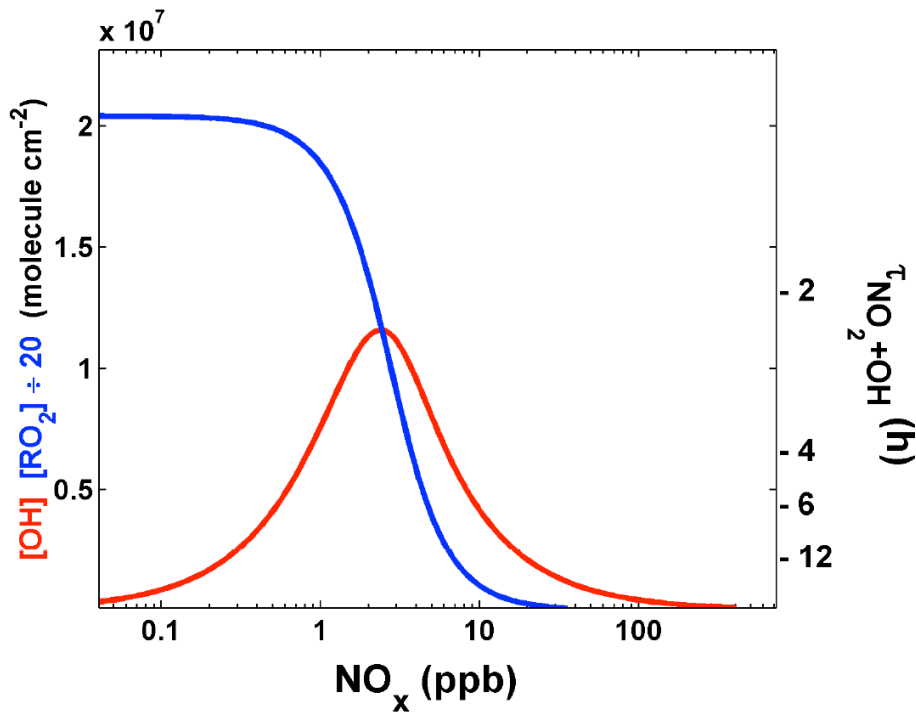


**Fig. 1.** The steady-state relationship of OH (red) and  $\text{RO}_2$  ( $\div 20$ ; blue) concentrations to the concentration  $\text{NO}_x$  using the relationship derived in Murphy et al. under conditions typical of a polluted summertime urban environment. The lifetime of  $\text{NO}_x$  with respect to reaction of  $\text{NO}_2$  with OH is indicated on the right axis.

**Urban scale spatial patterns of the  $\text{NO}_2$  Column**

L. C. Valin et al.

Title Page

Abstract

Introduction

Conclusions

References

Tables

Figures

◀

▶

◀

▶

Back

Close

Full Screen / Esc

Printer-friendly Version

Interactive Discussion



Urban scale spatial patterns of the NO<sub>2</sub> Column

L. C. Valin et al.

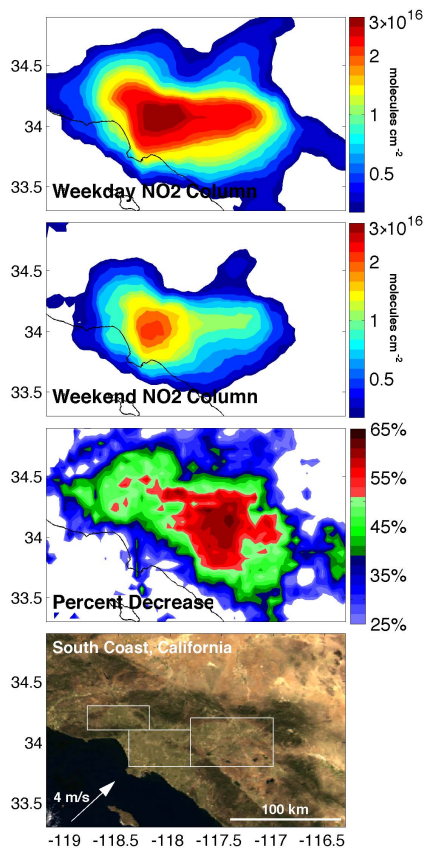


**Fig. 2.** May–July 2005–2007 average BEHR NO<sub>2</sub> column for weekdays (top panel) and weekends (second panel), and the percent weekend decrease (third panel). MODIS RGB image of Southern California (fourth panel) with the average North American Regional Reanalysis winds for the region (33.7°–34.0° N; 117.7°–118.4° W) reported in the bottom-left corner, and rectangles marking the San Fernando (NW), Los Angeles (SW) and San Bernardino (E) basins.

## Urban scale spatial patterns of the NO<sub>2</sub> Column

L. C. Valin et al.

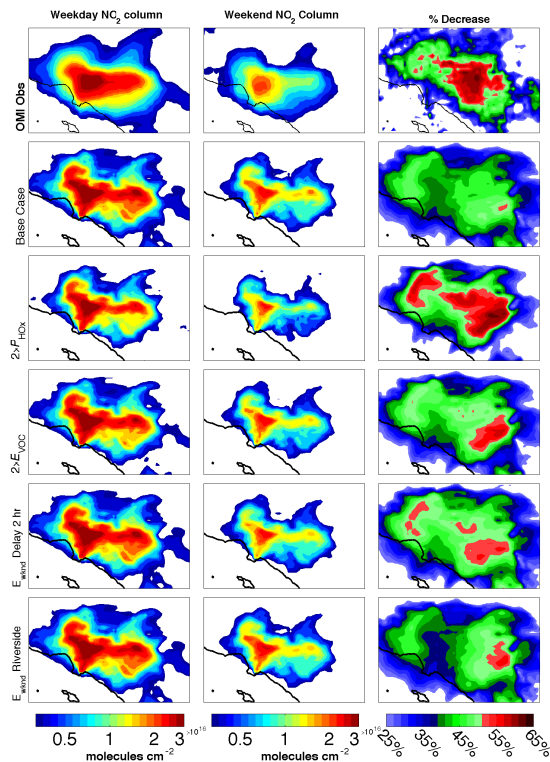


**Fig. 3.** Weekday NO<sub>2</sub> column, weekend NO<sub>2</sub> column, and percent change of NO<sub>2</sub> column (top row) observed by OMI for May–August 2005–2008, and simulated with WRF-Chem for 3–14 June 2008 at 1 p.m. LST using a uniform 37.5% reduction in NO<sub>x</sub> emissions with standard RADM2 chemistry (second row), a 2× increase of  $J_{O_3}$  (third row), a 2× increase of anthropogenic  $E_{VOC}$  (fourth row), a two-hour delay of anthropogenic weekend  $E_{NO_x}$  and  $E_{VOC}$  relative to weekdays (fifth row), and spatially distinct weekend  $E_{NO_x}$  reductions (sixth row; Weekend  $E_{NO_x-San\ Bernardino} = 0.525 \times E_{NO_x-NEI2005}$ , and  $E_{NO_x-Los\ Angeles} = 0.654 \times E_{NO_x-NEI2005}$ , such that the domain-average weekend  $E_{NO_x}$  is  $0.625 \times E_{NO_x-NEI2005}$ ).